Kinetic Mechanism of Human Hypoxanthine−Guanine Phosphoribosyltransferase: Rapid Phosphoribosyl Transfer Chemistry†

Yiming Xu,‡ Janina Eads,§ James C. Sacchettini,§,|| and Charles Grubmeyer*,‡

Department of Biochemistry and Fels Institute for Cancer Research and Molecular Biology, Temple University School of Medicine, 3420 North Broad Street, Philadelphia, Pennsylvania 19140, and Department of Biochemistry, Albert Einstein College of Medicine, 1300 Morris Park Avenue, Bronx, New York 10461

Received July 2, 1996; Revised Manuscript Received December 6, 1996⊗

ABSTRACT: Hypoxanthine−guanine phosphoribosyltransferase (HGPRTase) is the locus of Lesch-Nyhan syndrome, the activator of the prodrugs 6-mercaptopurine and allopurinol, and a target for antiparasitic chemotherapy. The three-dimensional structure of the recombinant human enzyme in complex with GMP has recently been solved [Eads, J., Scapin, G., Xu, Y., Grubmeyer, C., & Sacchettini, J. C. (1994) *Cell 78*, 325−334]. Here, ligand binding, pre-steady state kinetics, isotope trapping, and isotope exchange experiments are presented which detail the sequential kinetic mechanism of the enzyme. In the forward reaction, in which a base (hypoxanthine or guanine) reacts with PRPP to form nucleoside monophosphate and PP_i, binding of PRPP precedes that of the base, and in the reverse direction, IMP binds first. Compared to k_{cat}, phosphoribosyl group transfer is rapid in both the forward (131 vs 6.0 s^{-1}) and reverse (9 vs 0.17 s^{-1}) directions. In the forward direction, product pyrophosphate dissociates rapidly (>12 s^{-1}) followed by release of IMP (6.0 s^{-1}). In the reverse direction, Hx dissociates rapidly (9.5 s^{-1}) and PRPP dissociates slowly (0.24 s^{-1}). The more rapid rate of utilization of guanine than hypoxanthine in the forward reaction is the result of the faster release of product GMP rather than the result of differences in the rate of the chemical step. The kinetic mechanism, with rapid chemistry and slow product dissociation, accounts for the previously observed ability of the alternative product guanine to stimulate, rather than inhibit, the pyrophosphorolysis of IMP. The overall equilibrium for the hypoxanthine phosphoribosyl transfer reaction lies far toward nucleotide product ($K_{eq} \approx 1.6 \times 10^5$), at the high end for PRPP-linked nucleotide formation. The three-dimensional structure of the HGPRTase·IMP complex has been solved to 2.4 Å resolution and is isomorphous with the GMP complex. The results of the ligand binding and kinetic studies are discussed in light of the structural data.

Hypoxanthine−guanine phosphoribosyltransferase (HGPRTase,[1] EC 2.4.2.8) catalyzes the transfer of the 5-phosphoribosyl group from α-D-5-phosphoribosyl 1-pyrophosphate (PRPP) to hypoxanthine or guanine to form the nucleotide IMP or GMP, a critical reaction in purine salvage pathways.

$$\begin{matrix}\text{Hypoxanthine (Hx)}\\ \text{Guanine (Gua)}\end{matrix} + \text{PRPP} \underset{\leftarrow}{\overset{\text{HGPRTase}}{\rightarrow}} \begin{matrix}\text{IMP}\\ \text{GMP}\end{matrix} + \text{PPi}$$

The enzyme has a wide phylogenetic and tissue distribution and has been reported from the Gram-negative bacteria *Escherichia coli* and *Salmonella typhimurium* (Miller *et al.*, 1972; Hochstadt, 1978; Chou & Martin, 1972), the Gram-positive bacteria *Lactococcus lactis* (Nilsson & Lauridsen, 1992) and *Bacillus subtilis* (Ogasawara *et al.*, 1994), yeast (Kornberg *et al.*, 1955; de Groodt *et al.*, 1971), the parasitic worm *Schistosoma* (Dovey *et al.*, 1986), mammals (Korn *et al.*, 1955), and the parasitic protozoa *Leishmania* (Tuttle & Krenitsky, 1980) and *Plasmodium* (Queen *et al.*, 1988; Reyes *et al.*, 1982). In humans, HGPRTase is found in liver, red blood cells, and nervous tissues (Stout & Caskey, 1985). The complete lack of HGPRTase activity in humans causes the Lesch-Nyhan syndrome (Seegmiller *et al.*, 1967), characterized by hyperuricemia and neural disorders, including mental retardation and compulsive self-mutilation behavior (Lesch & Nyhan, 1964; Stout & Caskey, 1989), whereas partial deficiency of HGPRTase leads to gouty arthritis (Kelley *et al.*, 1967). Many pathogenic parasites, including *Schistosoma* and *Plasmodium*, lack *de novo* purine nucleotide synthesis and synthesize purine nucleotides only through salvage pathways. Therefore, HGPRTase has been proposed as a target for antiparasitic chemotherapy (Senft & Crabtree, 1983; Dovey *et al.*, 1984; Ullman & Carter, 1995).

Potent and specific inhibitors for parasitic HGPRTase must exploit structural and functional differences between the parasitic enzyme and its host counterpart. The crystal structure of the tetrameric human HGPRTase is now available (Eads *et al.*, 1994) and has revealed the architecture of the active site. A core α/β nucleotide binding motif is fused

† This work was supported by National Institues of Health Grant GM-52125.

* To whom correspondence should be addressed. Phone: 215-707-4495. Fax: 215-707-7536. E-mail: ctg@ariel.fels.temple.edu.

‡ Temple University School of Medicine.

§ Albert Einstein College of Medicine.

|| Current address: Center for Structural Biology, Department of Biochemistry and Biophysics, Texas A&M University, College Station, TX 77843.

⊗ Abstract published in *Advance ACS Abstracts,* March 1, 1997.

[1] Abbreviations: HGPRTase, hypoxanthine−guanine phosphoribosyltransferase; QAPRTase, quinolinic acid phosphoribosyltransferase; OPRTase, orotate phosphoribosyltransferase; NAPRTase, nicotinic acid phosphoribosyltransferase; XO, xanthine oxidase; PRPP, α-D-5-phosphoribosyl 1-pyrophosphate; OMP, orotidine monophosphate; NAMN, nicotinate mononucleotide; Hx, hypoxanthine; DTT, dithiothreitol; PTC, phenylthiocarbamyl.

S0006-2960(96)01600-5 CCC: $14.00

to a C-terminal β structure which appears to confer base specificity. A potential conformational change associated with base binding was identified in this C-terminal region. The structure of the active site also suggests that both PRPP and Hx should be able to bind simultaneously, consistent with chemical mechanisms involving direct transfer of the phosphoribosyl moiety within ternary complexes. A flexible loop, directly adjacent to the active site, may move to cover the active site during catalysis. It is not yet clear if the enzymes from parasites, which show 28−48% primary sequence identity with the human enzyme, demonstrate species specific structural differences, since only the crystal structure of the *Tritrichomonas foetus* enzyme is available (Somoza *et al*., 1996). Ullman and Carter (1995) have generated a molecular model of *Plasmodium* HGPRTase using the human HGPRTase structure as a template. The active site of this hypothetical structure is similar to that of the human enzyme. The structure of the schistosomal HGPRTase is especially anticipated since this enzyme is proposed to have an organization of the active site substantially different from that of the human enzyme (Kanaani *et al*., 1995).

Kinetic study has helped to elucidate the mechanism of action of phosphoribosyltransferases. Many of the phosphoribosyltransferases, including ATP-PRTase, OPRTase, and uracil PRTase, were reported to follow ping-pong type kinetic mechanisms, on the basis of parallel lines in steady state kinetic plots and/or catalysis of PRPP/PP_i or base/nucleotide isotope exchanges (Martin, 1963; Victor *et al.*, 1979; Natalini *et al*., 1979). Enzyme forms containing activated phosphoribose were proposed for ATP-PRTase (Bell & Koshland, 1970), adenine PRTase (Groth & Young, 1971), and OPRTase (Victor *et al.*, 1979). In some cases, these results have been shown to arise from experimental artifacts. For example, Brashear and Parsons (1975) demonstrated that ATP contamination in radiolabeled PRPP had led to the apparent detection of an enzyme-bound intermediate for ATP-PRTase. In the case of OPRTase, Bhatia *et al*. (1990) showed that OMP contamination of the enzyme and PP_i contamination of OMP led to artifactual exchange reactions. In that case, as with other PRTases, sequential kinetic mechanisms are more compatible with the available evidence. In accord with a sequential mechanism, an oxocarbonium-like transition state for direct phosphoribosyl transfer between PRPP and orotate in OPRTase has recently been delineated through the use of kinetic isotope effects (Tao *et al.*, 1996).

Prior kinetic studies on HGPRTase have been inconsistent in their conclusions. Henderson *et al.* (1968) in a characterization of the human enzyme concluded that HGPRTase followed a sequential kinetic mechanism, with ordered binding of PRPP and base, slow interconversion of ternary complexes, and ordered product release. Krenitsky and Papaioannou (1969) suggested that an alternative ping-pong pathway was also operative, a conclusion later put forward for the yeast enzyme (Ali & Sloan, 1982). Giacomello and Salerno developed a xanthine oxidase (XO)-coupled assay for the reverse pyrophosphorolysis reaction of the human enzyme and in a series of three papers (Giacomello & Salerno, 1978; Salerno & Giacomello, 1979, 1981) proposed a purely sequential kinetic mechanism for the reverse reaction with IMP and PP_i binding in rapid equilibrium random fashion, followed by phosphoribosyl transfer and ordered dissociation of Hx and PRPP. In the forward reaction, PRPP binding was proposed to precede binding of Hx, with random product release. A novel Gua/IMP exchange was interpreted to indicate slow release of PRPP from the E·PRPP complex (Salerno & Giacomello, 1979). Ali and Sloan (1982) used flow dialysis to identify a tight E·PRPP complex in the yeast enzyme, in agreement with kinetic mechanisms in which this substrate binds to the apoenzyme first. More recently, Yuan *et al.* (1992) employed steady state kinetics to show that the schistosomal enzyme follows an ordered kinetic mechanism, with PRPP binding followed by binding of Hx, and with release of PP_i preceding that of IMP. The studies to date were based nearly exclusively on steady state kinetics and are subject to the limitations and problems of interpretation that arise from those methods.

The availability of the recombinant enzyme makes it possible to employ techniques that are not feasible with the smaller quantities of protein available from tissue isolations. We report here the detailed kinetic mechanism for human HGPRTase determined using a combination of rapid quench, ligand binding, and isotope trapping experiments. We have clarified the sequential kinetic pathway, which is ordered in its associative steps, partially random in product dissociation, and which features rapid phosphoribosyl group transfer. We have also established rate constants for most of the individual steps.

MATERIALS AND METHODS

Materials. [8-^{3}H]Hypoxanthine and [8-^{14}C]guanine were obtained from Moravek Biochemicals, Inc. (Brea, CA). [γ-^{32}P]ATP was from Amersham. [^{32}P]PP_i was from Dupont NEN Research Products. Sheets of polyethyleneimine cellulose for thin layer chromatography (Macherey-Nagel Inc.) were from Alltech (Deerfield, IL). Econo-safe liquid scintillation cocktail was from Research Products International Corp. (Mt. Prospect, IL). Whatman 3MM paper and CF11 cellulose were obtained from Fisher. Charcoal (DARCO S-51 grade) was from ICI (Wilmington, DE). Yeast inorganic pyrophosphatase was from Boehringer-Mannheim Corp. DTT was from U.S. Biochemicals. Xanthine oxidase, PRPP, and other biochemicals were from Sigma Chemical Co. QAPRTase was prepared as described previously (Hughes *et al*., 1993).

[8-^{3}H]IMP was prepared enzymatically by incubating 50 μCi [8-^{3}H]Hx (12 Ci/mmol) at 30 °C for 30 min in 500 μL of 5 mM PRPP, 100 mM Tris-HCl, and 12 mM $MgCl_2$ at pH 7.4 with 3.2 μg of HGPRTase. The reaction mixture was then chromatographed using HPLC on a Waters μBondapak C_{18} column (3.9 × 300 mm) eluted isocratically with 1% acetonitrile in H_2O. The [8-^{3}H]IMP was found to be at least 99.8% pure as revealed by paper chromatography. [8-^{14}C]GMP was similarly prepared. For preparation of [β-^{32}P]PRPP, 30 μCi [γ-^{32}P]ATP (3 Ci/mmol) was included in 100 μL of 50 mM KH_2PO_4 and 50 mM triethanolamine at pH 8.0 containing 3 mM ribose 5-phosphate and 5 μg of *E. coli* PRPP synthase (Hove-Jensen *et al.*, 1986; a generous gift of R. Switzer). The reaction mixture was incubated at room temperature for 20 min before being applied to a 1 mL column of charcoal/CF11 cellulose (1:4, w:w; Parkin *et al.*, 1984) and eluted with 50 mM K_2HPO_4 at pH 8.0. Fractions containing [β-^{32}P]PRPP were collected and stored at −80 °C.

Enzyme Isolation. Recombinant human HGPRTase was expressed and purified as previously described (Eads *et al.*, 1994). The enzyme was homogeneous as judged by SDS-PAGE. The published extinction coefficient for human HGPRTase [E_{280}(1 mg/mL) = 0.53; Keough *et al.*, 1991] which was calculated on the basis of amino acid composition was carefully reexamined by quantitative amino acid analysis. Experiments were performed at the Protein Microchemistry Facility at the Wistar Institute (Philadelphia, PA). Samples were hydrolyzed with 6 N HCl and 1% phenol for 1 h at 160 °C in vapor phase, followed by manual PTC derivatization and HPLC separation essentially as described by Ebert (1986). Quantitative amino acid analysis gave a value for E_{280}(1 mg/mL) of 1.0. Protein was quantified spectrophotometrically using this revised value. The subunit molarity was calculated on the basis of an M_r of 24 470, calculated from the deduced protein sequence (Jolly *et al.*, 1983). The enzyme concentrations reported in this paper and used to calculate n and k_{cat} refer to the subunit concentration.

Standard Assays. The forward reactions catalyzed by HGPRTase, formation of IMP or GMP, were assayed at 30 °C using a Perkin-Elmer 552A UV/VIS spectrophotometer. The difference in extinction coefficients at 245 nm between IMP and Hx was determined to be 1900 M^{-1} cm^{-1} and was used to monitor the HPRTase forward reaction. The difference in extinction coefficients at 257.5 nm between GMP and Gua was determined to be 5900 M^{-1} cm^{-1} and was used to monitor the GPRTase forward reaction. The standard forward assay (1 mL) consisted of 100 μM Hx or Gua, 1 mM PRPP, 12 mM $MgCl_2$, and 100 mM Tris-HCl at pH 7.4. The reverse reaction (IMP pyrophosphorolysis) was assayed either spectrophotometrically or by using a radiolabel transfer method at 30 °C . The spectrophotometric assay employed xanthine oxidase (XO). Assay components consisted of 100 μM IMP, 500 μM PP_i, 5 mM $MgCl_2$, 0.1 unit of XO, and 100 mM Tris-HCl at pH 7.4 in a final volume of 1 mL. The formation of uric acid was monitored using an extinction coefficient of 12 000 M^{-1} cm^{-1} at 293 nm (Kalckar, 1947). In the radiolabel transfer method, the reverse reaction was assayed with [8-^{3}H]IMP or [8-^{14}C]GMP. A typical assay (in 0.1 mL) included 100 μM [8-^{3}H]IMP or [8-^{14}C]GMP (0.08 μCi), 500 μM PP_i, 5 mM DTT, and 5 mM $MgCl_2$ in 100 mM Tris-HCl at pH 7.4. Products [^{3}H]-Hx and [^{3}H]IMP (or [^{14}C]Gua and [^{14}C]GMP) were resolved by paper chromatography, on Whatman 3 MM paper developed in 400 mM Na_2HPO_4 (pH 8.0) of 10 μL samples of reaction mixture (Henderson *et al.*, 1968). The radiolabel transfer method was used to determine the apparent K_{eq} for IMP pyrophosphorolysis. The reaction mixture consisted of either 0.1 or 1 mM [8-^{3}H]IMP, 20 mM PP_i, 20 mM $MgCl_2$, and 5 mM DTT in 100 mM Tris-HCl at pH 7.4. The conversion of IMP to Hx was analyzed by paper chromatography at various times from 0 to 50 min.

Analysis of Kinetic Data. Steady state kinetic parameters (k_{cat} and K_m) were evaluated with the HYPER program of Cleland (1979) and are reported ± standard errors.

Rapid Quenching Experiments. Pre-steady state kinetic experiments were performed at room temperature (22−24 °C) in a Precision Syringe Ram, model 1010 (Update Instrument Inc., Madison, WI). A two-syringe setup was used. A typical reaction was started by mixing 50 μL of solution from each syringe and ejecting from the aging hose through a nozzle into 400 μL of 0.6−0.9 N $HClO_4$. When reaction times greater than 200 ms were desired, a two-push protocol was employed. The mixture was centrifuged to precipitate denatured enzyme. The pH of the supernatant was brought to approximately pH 7 with 6 N KOH, cooled on ice, and the $KClO_4$ precipitate was then removed by centrifugation. The supernatant was injected onto a Waters μBondapak C_{18} column (3.9 × 300 mm) and eluted isocratically with either 100 mM $(NH_4)_2HPO_4$ at pH 5.0 or 1% acetonitrile in H_2O. Chromatographic peaks containing base and nucleotide, monitored at 206 nm, were collected, and the radioactivity was measured by liquid scintillation. Controls were performed in which 50 μL of solution from the syringe that contained HGPRTase was thoroughly mixed with 400 μL of $HClO_4$ followed by addition of 50 μL of solution from the other syringe. The mixture was then treated according to the aforementioned procedures. No residual enzymatic activity was detected, indicating that the denaturation procedure was effective.

Equilibrium Gel Filtration. The approach of Hummel and Dreyer (1962), as modified by Grubmeyer *et al.* (1987), was used to quantitate ligand binding. HGPRTase was equilibrated with [β-^{32}P]PRPP and [^{3}H]glucose in 100 μL of 100 mM Tris-HCl, 12 mM $MgCl_2$, and 5 mM DTT at pH 7.4 for 10 min at room temperature. The mixture was then applied to Sephadex G-50 in a 1 mL tuberculin syringe preequilibrated and eluted with [β-^{32}P]PRPP and [^{3}H]glucose in the same buffer. Fifty single-drop fractions were collected in 4 mL Wheaton Omni-Vials. Counting by liquid scintillation was conducted until 1% error was reached in both the ^{3}H and ^{32}P channels, and standards were used to correct for spillover of ^{32}P into the ^{3}H channel. The counts in the ^{3}H channel were then used to calculate the volume of each drop, and the average of the total excess ^{32}P present in the peak fractions and deficient in the trough fractions was used to calculate bound [β-^{32}P]PRPP. Determinations of bound and bound/free were plotted (Scatchard, 1949) and fit by linear least squares.

Isothermal Titration Calorimetry of Nucleotide Binding to HGPRTase. The experiments were performed using an isothermal titration calorimeter (MicroCal, Inc., Northampton, MA). Twenty-five 4 μL injections of 3−10 mM nucleotides (IMP or GMP) in 20 mM Tris-HCl, 12 mM $MgCl_2$, and 1 mM DTT at pH 8.0 were made into 1.4 mL of 53−132 μM HGPRTase in the same buffer at 27 °C. As noted, in some cases, $MgCl_2$ was absent. MicroCal software was used to fit the data using a nonlinear least-squares algorithm. The errors reported here are those generated by the MicroCal fitting program and reflect the quality of the fit of the data to the titration curve.

Equilibrium Dialysis. A multisample Microvolume Dialyzer (model EMD 101B, Hoefer Scientific Instruments, San Francisco) was used in equilibrium dialysis. To measure the binding of Hx to apoenzyme, 200 μL of 151 μM HGPRTase subunit, 4.1 μM [^{3}H]Hx, 100 mM Tris-HCl, 12 mM $MgCl_2$, and 5 mM DTT at pH 7.4 was injected into one side of the dialyzer chamber and 200 μL of the same solution without HGPRTase was injected into the opposite side. The two chambers were separated by a sheet of dialysis membrane with a nominal molecular mass cutoff of 12−14 kDa (Hoefer). For measurement of PP_i binding, 200 μL of 245 μM HGPRTase, 60 μM [^{32}P]PP_i, 100 mM Tris-HCl, 12 mM $MgCl_2$, and 5 mM DTT at pH 7.4 and the same solution without HGPRTase were loaded into the two chambers.

Hypoxanthine (2.2 mM) was also added in studies of the E·PP_i·Hx dead-end complex. In all cases, the samples were incubated with constant mixing at room temperature for ca. 12 h. An aliquot of sample was then taken from each chamber and the radioactivity determined by liquid scintillation.

Isotope Trapping. The experiments were performed at room temperature. For isotope trapping with [β-^{32}P]PRPP, 10 μL of an equilibrium binding mixture containing 14.2 μM HGPRTase, 22.2 μM [β-^{32}P]PRPP in 50 mM KP_i, and 4.6 mM $MgCl_2$ at pH 7.5 was injected into 450 μL of rapidly stirred chase solution (190 μM Hx, 1.58 mM PRPP, 50 mM KP_i, and 5 mM $MgCl_2$ at pH 7.5), using a Hamilton syringe. Five seconds (30 turnovers) after mixing, 100 μL of 500 mM EDTA was added. A sample (15 μL) of EDTA-quenched mixture was applied on a polyethyleneimine cellulose film and chromatographed with 2 M LiCl and 100 mM Tris-HCl at pH 8.0. A phosphorimager screen was exposed to the chromatogram. Using a BAS2000 Fujix Bioimaging analyzer (Fuji Photo Film Co., Ltd.), [^{32}P]PRPP and [^{32}P]PP_i spots were identified with standards, and the digitized, background-corrected, photostimulated luminescence was quantified. To measure isotope trapping of [^{3}H]-IMP, the equilibrium binding mixture contained 73 μM HGPRTase, 0.4 μM [^{3}H]IMP in 100 mM Tris-HCl, 5 mM DTT, and 5 mM $MgCl_2$ at pH 7.4. A portion (10 μL) was injected into 933 μL of 1.5 mM IMP, 200 μM Hx, 20 mM PP_i, and 25 mM $MgCl_2$ in 100 mM Tris-HCl at pH 7.4 (chase solution). After 30 s of reaction (5 turnovers), 67 μL of 9 N $HClO_4$ was added, and quenched samples were processed as for rapid quenching experiments. To ensure that the isotopic dilution was sufficient, controls were carried out in which 10 μL of apoenzyme HGPRTase was injected into 450 μL of chase solution which also contained radiolabeled PRPP or IMP. Control samples were processed as described for experimental samples.

HGPRTase·IMP Crystallization and Structure Determination. Crystals of HGPRTase complexed with IMP were produced under conditions identical to those reported for the complex of HGPRTase with GMP (Eads *et al*., 1994). Crystals grew to maximum dimensions of 0.5 × 0.5 × 0.2 mm and diffracted to a maximum resolution of 2.2 Å. Data were collected from two crystals, using a pair of Xuong-Hamlin multiwire detectors and a Rigaku RU-200 rotating anode as the X-ray source. Data were collected and processed using the software supplied with the detectors (C. Nielsen, San Diego Multiwire).

RESULTS

Properties of Recombinant HGPRTase. The purification of recombinant human HGPRTase from the T7 promoter-driven pYM10 clone was similar to that described previously (Eads *et al.*, 1994) except that, after the initial precipitation with 60% saturation $(NH_4)_2SO_4$, samples were first subjected to chromatography on the Q-Sepharose column (HiLoad 26/10, Pharmacia) followed by the Phenyl-Sepharose column (HiLoad 16/10, Pharmacia). Amino acid sequencing of the recombinant HGPRTase revealed that the initiator methionine had been removed, as in mature human erythrocyte HGPRTase (Wilson *et al*., 1982). Gel filtration of the enzyme (0.38 mg/mL) on a Superdex-200 column (HiLoad 16/60, Pharmacia) indicated that it was tetrameric in 100 mM Tris-HCl, 0.1 mM EDTA, 1 mM DTT, and 10% glycerol at pH 7.4, which is also consistent with previously reported results (Holden & Kelley, 1978).

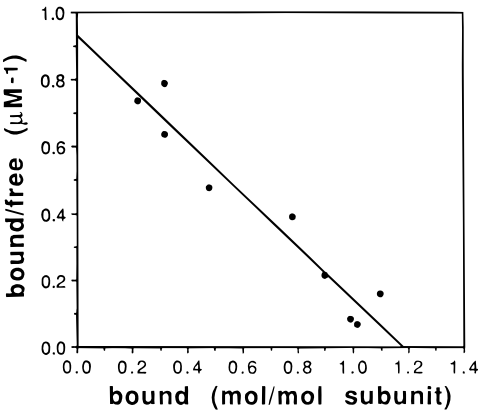

FIGURE 1: Scatchard plot of binding of [β-^{32}P]PRPP to HGPRTase. The data are from equilibrium gel filtration experiments as described in Materials and Methods. HGPRTase and [β-^{32}P]PRPP were used at 0.26−2.6 and 0.3−30 μM, respectively. The line represents the linear least-squares fit.

Values for V_{max} and K_m were determined using spectrophotometric assays at 30 °C. The specific activity of the pure recombinant human HGPRTase, ranging from 21 to 23 μmol of IMP formed min^{-1} mg^{-1} (k_{cat} = 8.5−9.3 s^{-1}) at 30 °C, was similar to reported values (Muensch & Yoshida, 1977; Olsen & Milman, 1977). At room temperature (22−24 °C), the specific activity was 14−15 μmol of IMP formed min^{-1} mg^{-1} (k_{cat} = 5.7−6.4 s^{-1}). The specific activity in the reverse reaction was 0.57−0.76 μmol of Hx formed min^{-1} mg^{-1} (k_{cat} = 0.23−0.30 s^{-1}) at 30 °C and 0.34−0.53 μmol of Hx formed min^{-1} mg^{-1} (k_{cat} = 0.13−0.21 s^{-1}) at room temperature. As noted by others (Keough *et al.*, 1991; Yuan *et al.*, 1992), Gua was utilized more rapidly than Hx, with a V_{max} of 43 μmol of GMP formed min^{-1} mg^{-1} (k_{cat} = 18 s^{-1}) at 30 °C. The K_m values for Hx (2.4 ± 0.6 μM), PRPP (35 ± 6 μM with Hx as the second substrate, 65 ± 6 μM with Gua as the second substrate), Gua (3.5 ± 1.2 μM) IMP (5.4 ± 1.2 μM), and PP_i with IMP as second substrate (25 ± 8 μM), were similar to those published for the human enzyme purified from erythrocytes (Giacomello & Salerno, 1978) or adenocarcinoma cells (Hill, 1970).

Substrate Binding. Experiments were performed to investigate the order of the binding of substrates to HGPRTase. Binding of [β-^{32}P]PRPP (Figure 1) was measured by equilibrium gel filtration. The results fit well to a model with a single class of homogeneous binding sites indicating that PRPP binds to the apoenzyme with a K_D of 1.3 ± 0.1 μM and an n of 1.18 ± 0.06 mol of PRPP/(mol of HGPRTase subunit) [4.6 mol/(mol of tetramer)]. When [β-^{32}P]PRPP binding experiments were performed in the absence of Mg^{2+}, no binding was detected. Inclusion of IMP reduced the amount of [β-^{32}P]PRPP bound to the enzyme, allowing calculation of the K_D for IMP of 53 μM. Pyrophosphate at 1.5 mM did not detectably compete with [β-^{32}P]PRPP for binding to the enzyme, suggesting that PP_i binds poorly to the apoenzyme. On the basis of the detection limits of the procedures, if PP_i does bind to the apoenzyme, it must have a K_D of at least 7.5 mM.

Binding of IMP to the apoenzyme in the presence of Mg^{2+} was also quantitated directly by isothermal titration calorimetry (Figure 2). The data were fit to a single-binding

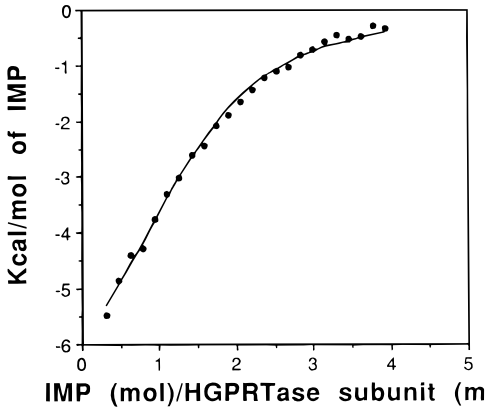

FIGURE 2: Isothermal titration of IMP binding to HGPRTase. Each point represents an injection of IMP. The molar ratio refers to the ratio of cumulative IMP concentration to total HGPRTase subunit concentration. The *y*-axis represents enthalpy change brought by each injection. The line represents the fit using a nonlinear least-squares alogrithm.

site model which yielded a K_D of 61 ± 6 μM and an *n* of 1.32 ± 0.06 mol of IMP/(mol of subunit) [5.3 mol/(mol of tetramer)]. GMP binding experiments using the same method gave a K_D of 7.1 ± 0.2 μM, with an *n* of 1.27 ± 0.02 mol of GMP/(mol of subunit) [5.0 mol/(mol of tetramer)] (data not shown). When Mg^{2+} was omitted, the K_D for GMP was 3.2 ± 0.3 μM with an *n* of 1.27 ± 0.02 mol of GMP/(mol of subunit) [5.0 mol/(mol of tetramer)], and the K_D for IMP was 39 ± 3 μM with an *n* of 1.00 ± 0.04 mol of IMP/(mol of subunit) [4.0 mol/(mol of tetramer)]. At 200 μM, weak binding of [8-^{14}C]guanine to the apoenzyme was detected by equilibrium dialysis. Accurate determination of a K_D for guanine was prevented by its low solubility, but the results suggested a K_D of ≥ 300 μM. No binding of either Hx or PP_i to the apoenzyme was detected by isothermal titration calorimetry, equilibrium dialysis, or, as determined only for Hx, equilibrium gel filtration. On the basis of the sensitivity of the techniques employed, it was possible to estimate the lower limit of K_D values for Hx and PP_i. K_D values for the binding of these ligands to the apoenzyme must be at least 1.9 mM for Hx and 1.8 mM for PP_i, if binding does occur.

Isotope trapping experiments (Rose, 1980, 1995) were carried out to quantitate the behavior of the binary complexes for each of the two substrates that bind to the apoenzyme, PRPP and IMP. In these experiments, an equilibrium binding mixture of enzyme and radioactive substrate was injected into a solution containing the second substrate and a large molar excess of nonradioactive substrate. Mixtures (10 μL) of 14.2 μM enzyme and 22.2 μM [β-^{32}P]PRPP, in which 64% of the [β-^{32}P]PRPP was calculated to be bound, were injected into a trapping solution (450 μL) containing 190 μM Hx and 1.58 mM nonradioactive PRPP. After 5 s (30 turnovers), the reaction was quenched. Of the [β-^{32}P]-PRPP present, 73.5 ± 8.3% (115% of the [β-^{32}P]PRPP calculated to be bound) was converted to [^{32}P]PP_i. Controls showed that only 0.1% of conversion of previously unbound [β-^{32}P]PRPP to [^{32}P]PP_i occurred in the trapping solution, indicating effective dilution of [β-^{32}P]PRPP by a nonradioactive compound. The results confirm that enzyme-bound [β-^{32}P]PRPP is catalytically competent. When similar experiments were performed with mixtures of 73 μM enzyme and 0.4 μM [^{3}H]IMP, only 5% of the [^{3}H]IMP calculated to be bound to the enzyme was found to be trapped as [^{3}H]Hx

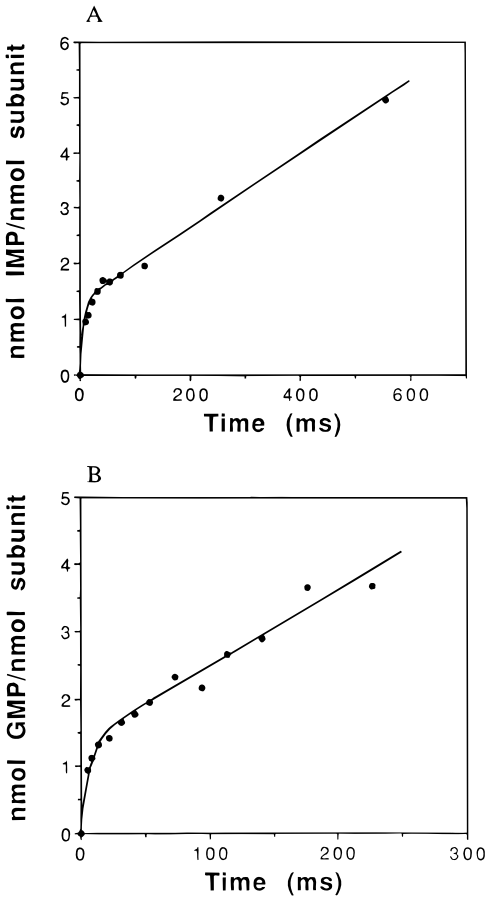

FIGURE 3: Pre-steady state nucleotide formation by HGPRTase. (A) IMP formation. One syringe contained [^{3}H]Hx in 100 mM Tris-HCl, 12 mM $MgCl_2$, and 5 mM DTT at pH 7.4. The other syringe contained HGPRTase and PRPP in the same buffer. Reactions were initiated when equal volumes of solution from each syringe were mixed in the mixer. The final concentrations of HGPRTase, Hx, and PRPP were 4.7 μM, 100 μM, and 1 mM, respectively. Reaction samples were processed [100 mM $(NH_4)_2HPO_4$ at pH 5.0 was used as the solvent] as described in Materials and Methods. (B) GMP formation. Conditions were as for panel A except [^{14}C]Gua replaced [^{3}H]Hx. The final concentrations were 5.4 μM HGPRTase, 105 μM Gua, and 1 mM PRPP. Acetonitrile (1%) in H_2O was used as the solvent in chromatography. The lines in panels A and B represent the best fit as described in Results.

in solutions containing 20 mM PP_i, whereas the remaining 95% of the bound [^{3}H]IMP dissociated without undergoing net conversion to [^{3}H]Hx. The high level of PP_i employed ensured that all E·[^{3}H]IMP would be converted to the E·[^{3}H]-IMP·PP_i ternary complex. The ability to trap only 5% of the bound [^{3}H]IMP is thus most likely due to the release of [^{3}H]IMP from the E·[^{3}H]IMP·PP_i ternary complex. Efforts to trap an E·[^{3}H]Hx complex with PRPP were unsuccessful, providing a further indication that Hx binds poorly to the apoenzyme. On the basis of the results of binding and isotope trapping experiments, ordered binding of substrates is indicated. In the forward direction, PRPP binds first, whereas IMP binds first in the reverse reaction.

Phosphoribosyl Group Transfer. When [^{3}H]IMP formation from [^{3}H]Hx in the forward reaction was monitored using a rapid quenching apparatus, a biphasic time course was obtained (Figure 3A) which consisted of an initial rapid phase followed by a slower linear phase. The linear phase represented steady state formation of [^{3}H]IMP with a k_{cat} of 6.6 s^{-1}, a value identical to that measured for the same enzyme preparation in the spectrophotometric assay at the

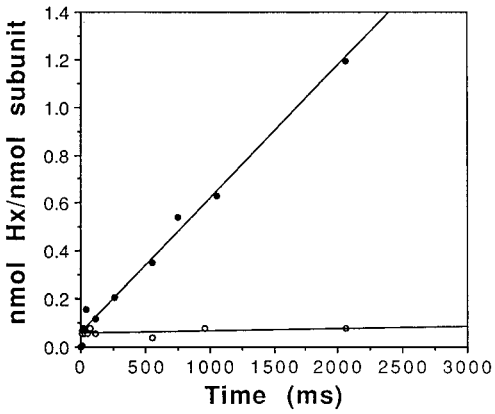

FIGURE 4: Pre-steady state kinetics of IMP pyrophosphorolysis. (○) One syringe contained PP_i in 100 mM Tris-HCl and 5 mM DTT at pH 7.4. The other syringe contained [^{3}H]IMP and HGPRTase in 100 mM Tris-HCl, 10 mM $MgCl_2$, and 5 mM DTT at pH 7.4. The final concentrations of HGPRTase, IMP, and PP_i were 5.7 μM, 100 μM, and 1 mM, respectively. The reaction samples were treated as for Figure 3B. (●) The conditions were the same as those for ○ except that nonradioactive Hx was included giving a final concentration of 100 μM. The lines represent the linear least-squares fit.

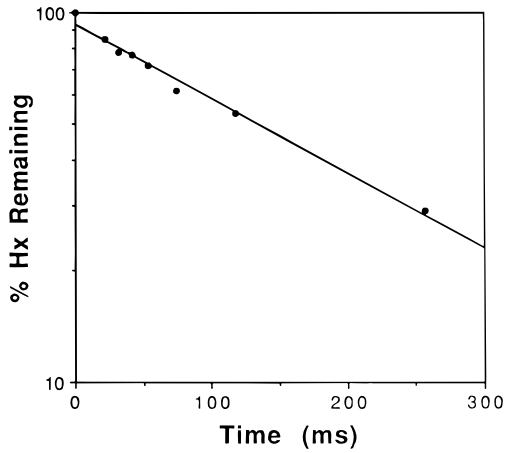

FIGURE 5: Measurement of k_{on} for Hx binding to the E·PRPP complex. The E·PRPP complex was formed by incubating 540 nM HGPRTase with 2 mM PRPP in one syringe. The other syringe contained 88 nM [^{3}H]Hx. The experimental procedures were the same as those in Figure 3A. The line represents the linear least-squares fit.

same temperature (23 °C). The entire data set was fit to the following equation (eq 1):

$$[\text{mol of IMP formed/(mol of total subunit)}] = n(1 - e^{-k_{obs}t}) + k_{cat}t \quad (1)$$

where k_{obs} is the first-order rate constant for the rapid phase and n represents the size of the burst of [^{3}H]IMP formation [mol of [^{3}H]IMP/(mol of enzyme subunit)] when the steady state phase was extrapolated to zero time. The value of n was 1.2−1.3 mol of [^{3}H]IMP/(mol of subunit). In simulations, fitting was attempted with values of k_{obs} from 20 to 300 s^{-1}. The best fit was obtained with a k_{obs} of 140 s^{-1} and was constant among experiments. The pre-steady state kinetics clearly demonstrated that, in the forward reaction, the formation of enzyme-bound IMP is fast relative to the release of the products. Similar results were obtained when [^{14}C]Gua was used as the base substrate (Figure 3B) with a rapid phase (k_{obs} = 140 s^{-1}) followed by a linear phase (k_{cat} = 11 s^{-1}) which was comparable to a k_{cat} of 13 s^{-1} measured with the spectrophotometric assay at room temperature. The burst of [^{14}C]GMP formed was 1.3 mol of [^{14}C]GMP/(mol of subunit).

When similar pre-steady state kinetic experiments for the reverse IMP pyrophosphorolysis reaction were carried out, no continuing net product formation was detected (Figure 4). However, if non-radiolabeled Hx was added to the reaction mixture to isotopically dilute released [^{3}H]Hx, a steady state conversion of labeled [^{3}H]IMP to [^{3}H]Hx could be easily monitored. Under either set of conditions, extrapolation to zero time showed a small burst of [^{3}H]Hx production [n = 0.085 mol of [^{3}H]Hx/(mol of subunit)]. The ratio of burst sizes is thus 1.3/0.085 = 15 which represents the equilibrium constant for the interconversion of ternary enzyme−substrate and enzyme−product complexes. The first-order rate constant describing the pre-steady state burst (140 s^{-1}) is the sum of the forward and reverse rate constants (Fersht, 1985).

$$k_{obs} = k_f + k_r$$

The ratio of the burst size in the forward and reverse directions allows the calculation of the rate constants for the interconversion of E·Hx·PRPP and E·IMP·PP_i with rates of 131 and 9 s^{-1} in the forward and reverse directions, respectively.

A minimal on rate for Hx binding to the E·PRPP complex was determined by rapid quench experiments with 270 nM HGPRTase subunit and 44 nM [^{3}H]Hx, in the presence of 1 mM PRPP (Figure 5). Under these conditions, pseudo-first-order conversion of [^{3}H]Hx to [^{3}H]IMP was observed, allowing calculation of the Hx on rate (1.7×10^7 M^{-1} s^{-1}). The experiment was repeated with 0.05 and 5.6 μM HGPRTase. The mean value for the Hx on rate was (1.9 ± 0.3) $\times 10^7$ M^{-1} s^{-1}.

Product Release. The overall rate of the reverse reaction, 0.17 s^{-1}, is far slower than the rate of the reverse phosphoribosyl transfer step, 9 s^{-1}, suggesting that Hx or PRPP release is rate-limiting in the reverse reaction. If PRPP release were slow, then given the rapid rate of Hx binding and the rapid forward phosphoribosyl transfer, a long-lived E·PRPP complex should be able to bind base to catalyze a rapid exchange reaction under conditions of reverse catalysis (exchange against the flow; Cho *et al.*, 1988). We were able to detect and quantitate a [^{3}H]Hx/IMP exchange reaction proceeding at 1.1 s^{-1}, about 6 times faster than net reverse catalysis. Previously, Salerno and Giacomello (1979) detected acceleration of IMP pyrophosphorolysis in the presence of guanine. We were able to confirm this observation by spectrophotometric assays and determined a rate for the guanine-accelerated IMP pyrophosphorolysis of 0.57 s^{-1}. As observed by Salerno and Giacomello (1979), the stimulation of IMP pyrophosphorolysis by Gua was transitory and was accompanied by formation of an amount of GMP stoichiometric to the amount of guanine added (not shown). The guanine-stimulated IMP pyrophosphorolysis reaction is thus a mixed Gua/IMP exchange, diagnostic of mechanisms in which release of a second product is slow (Segel, 1975). Since the conversion of E·Gua·PRPP to free GMP is rapid (13 s^{-1}), the exchange rate (k_{ex}) represents the net rate constant (Cleland, 1975) for the conversion of E·IMP·PP_i to E·PRPP. The equations below (eqs 2−4) describe the relationships between individual rate constants and k_{cat} for

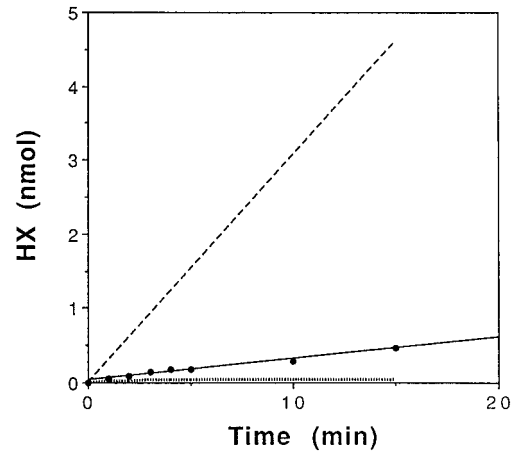

FIGURE 6: Reverse HGPRTase reaction coupled to QAPRTase. The reaction mixture consisted of 100 μL of 100 μM [^{3}H]IMP, 500 μM PP_i, 400 μM QA, 5 mM $MgCl_2$, 5 mM DTT, and 100 mM Tris-HCl at pH 7.4 containing 0.53 μg (0.0003 unit) of HGPRTase and 0.02 unit of QAPRTase at 30 °C. At the indicated times, 10 μL of the reaction mixture was sampled and analyzed as described in Materials and Methods. The solid line represents the linear least-squares fit of the data. The dashed line represents the rate of the reverse reaction in separate experiments in which xanthine oxidase replaced QAPRTase. The dotted line represents the rate of the reverse reaction when neither xanthine oxidase nor QAPRTase was present.

the reverse reaction and k_{ex}.

$$1/k_{-1} + 1/k_{-2} + 1/k'_{-3} = 1/k_{\text{cat (reverse)}} \quad (2)$$

$$1/k_{-2} + 1/k'_{-3} = 1/k_{ex} \quad (3)$$

$$k'_{-3} = k_{-3}k_{-2}/(k_3 + k_{-2}) \quad (4)$$

where k'_{-3} refers to the net rate constant for the step k_{-3} (see Scheme 1 in the Discussion for nomenclature). Equations 2−4 allow the calculation of the rate constant for Hx release from the E·PRPP·Hx complex (k_{-2}), 9.5 s^{-1}, and that for PRPP release from the E·PRPP complex (k_{-1}), 0.24 s^{-1}.

Xanthine oxidase (XO), which converts Hx to uric acid, was required to observe the net reverse reaction catalyzed by HGPRTase (Giacomello & Salerno, 1978). We performed experiments in which XO was replaced by quinolinic acid PRTase (QAPRTase), which serves to remove PRPP instead of Hx. A level of QAPRTase sufficient to produce maximal HGPRTase reaction rates was employed. Under these conditions, the reverse reaction gave linear production of Hx at a rate (0.019 s^{-1}) 10-fold less than that obtained when coupled to XO (Figure 6). The addition of QAPRTase to control assays containing XO did not affect the observed rate. The slower rate observed when QAPRTase, rather than XO, was used as the coupling enzyme is best explained by the random release of Hx and PRPP from the ternary E·Hx·PRPP complex. In the presence of XO, direct release of Hx from this complex (9.5 s^{-1}) is 40-fold faster than the release of PRPP (0.24 s^{-1}), making primary Hx release the favored pathway. However, when free Hx is not removed from the reaction, it rebinds to the E·PRPP complex (k_{on} = 1.9 × 10^7 M^{-1} s^{-1}), forcing the release of PRPP from the E·PRPP·Hx complex to be the predominant route for net product release. The result also strongly favors the idea that the reverse HGPRTase reaction is thermodynamically disfavored, since at least one of the products must be depleted in order to detect net reverse reaction.

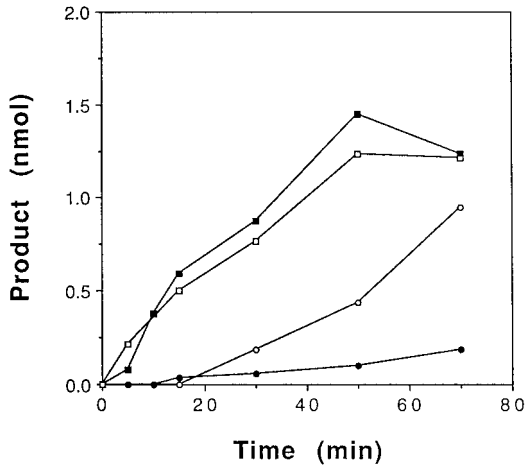

FIGURE 7: Time course of formation of [^{14}C]Gua (circles) and [^{3}H]-IMP (squares) at 30 °C. All reaction mixtures consisted of 100 μL of 200 μM Hx, 19 μM PRPP, 100 μM GMP, 5 mM $MgCl_2$, and 50 mM K_2HPO_4 at pH 7.5 containing 0.79 μg of HGPRTase. To measure formation of [^{14}C]Gua, a trace amount of [^{14}C]GMP was added. To measure formation of [^{3}H]IMP, a trace amount of [^{3}H]-Hx was included. The reaction mixtures were incubated either without pyrophosphatase (open symbols) or with 0.2 unit of pyrophosphatase (filled symbols). Samples (10 μL) of reaction mixtures were analyzed at the indicated times as described in Materials and Methods.

The order of release of IMP and PP_i from the enzyme·PP_i·IMP complex was investigated by monitoring the time course of [^{14}C]Gua formation from [^{14}C]GMP in reaction mixtures containing HGPRTase, Hx, PRPP, and [^{14}C]GMP, with or without added inorganic pyrophosphatase (Figure 7). If IMP can dissociate from the E·IMP·PP_i complex before PP_i, then free [^{14}C]GMP should be able to bind to the E·PP_i complex to form and release [^{14}C]Gua. The inclusion of pyrophosphatase should thus have little effect. However, if PP_i dissociation precedes IMP dissociation, then the inclusion of pyrophosphatase should prevent [^{14}C]Gua formation. Formation of [^{14}C]Gua from [^{14}C]GMP was observed in the absence of pyrophosphatase, but only following an initial lag phase. The reaction was almost totally abolished by the inclusion of pyrophosphatase. To assure that continuous conversion of Hx to IMP was occurring under these experimental conditions, the formation of [^{3}H]IMP from [^{3}H]-Hx was also measured under identical conditions in separate experiments. Pyrophosphatase did not affect the rate of formation of [^{3}H]IMP. These observations suggest that the conversion of [^{14}C]GMP to [^{14}C]Gua under these conditions required free PP_i, consistent with PP_i release preceding release of IMP in the forward reaction.

Dead-End E·Hx·PP_i Complex. It has been shown by other workers that PP_i is a good inhibitor of the forward reaction, competitive with respect to PRPP (Giacomello & Salerno, 1978). With the use of the spectrophotometric assay, we were able to confirm that PP_i inhibition of the recombinant human HGPRTase occurred and was indeed competitive with respect to PRPP (K_I = 240 ± 33 μM). However, we were unable to detect the binding of [^{32}P]PP_i to free enzyme, suggesting that an E·Hx·PP_i dead-end complex might form. Indeed, when Hx was present at 2.2 mM, with [^{32}P]PP_i at 100 μM and HGPRTase at 148 μM, equilibrium dialysis revealed that 22 μM [^{32}P]PP_i was bound to HGPRTase. Precipitation of the Mg_2PP_i complex at high PP_i levels precluded accurate determination of the K_D for PP_i from the dead-end complex.

Table 1: Summary of Data Collection and Crystal Parameters for HGPRTase·IMP

resolution range	∞−2.38 Å
R_{symm}	8.8%
completeness	77% (55% in the 2.6−2.4 Å shell)
	14 252 reflections > 1σ in the 20−2.4 Å range (77%)
unit cell	a = 129.3 Å, b = 66.4 Å, c = 52.9 Å, and $\alpha = \beta = \gamma = 90°$
space group	$P2_12_12$

Equilibrium Constant. The PRTase reactions display a wide range of external K_{eq} values, from 0.1 for OPRTase (Bhatia *et al*., 1990), and 0.67 for NAPRTase (Vinitsky & Grubmeyer, 1993), to a value of 300 for adenine PRTase (Hori & Henderson, 1966). Attempts to measure the external K_{eq} for the HGPRTase reaction provided only estimated values. The method of Purich and Allison (1983) with spectrophotometric observation of IMP/Hx ratios at 245 nm did not provide accurate data at high product/substrate ratios. However, when the reverse reaction was run to apparent equilibrium (50 min at room temperature with [^{3}H]IMP in the absence of any coupling system), the external K_{eq} was estimated to be 1.8-4.3 × 10^5.

Structure of the HGPRTase·IMP Complex. The results of data collection are summarized in Table 1. The crystals of the IMP complex were essentially isomorphous with respect to those of the GMP complex; thus, the structure was solved using the HGPRTase·GMP coordinates (Eads *et al*., 1994) as the initial model, with no ligand or ordered water. Rigid body refinement using least-squares methods (TNT; Tronrud *et al*., 1988) reduced the *R*-factor from 25.4 to 24.3%. Subsequently, least-squares refinement with restrained individual temperature factor refinement reduced the *R*-factor to 19.4% with good geometry. Electron density maps ($|F_o| - |F_c|$) clearly showed the location of the bound ligand and also clearly showed that there was no electron density at the position occupied by the N2 amino group of GMP. Addition of the IMP ligand and ordered water molecules into the model, with manual model building using TOM (Jones, 1985), was followed by further least-squares refinement. The final model contains 3259 of 3424 non-hydrogen protein atoms, two IMP molecules, and 65 ordered water molecules and has an *R*-factor of 17.8%, with rms deviation from ideal geometry of 0.019 Å for bond lengths and 2.5° for bond angles.

The structure of the HGPRTase·IMP complex was essentially identical to the structure of the HGPRTase·GMP complex (Figure 8). Minor differences include the positioning of the Lys-68 side chain, whose dissimilar conformations in the two complexes may reflect disorder of this residue. Side chain positions at the exterior of the protein and the positions of residues in the poorly defined loop region of residues 100−125 (Eads *et al*., 1994) also vary between the two complexes (not shown). There was no evidence for an ordered water molecule in the position occupied by the N2 amino group in the HGPRTase·GMP complex. The average temperature factor of the bound IMP was significantly higher than the average temperature factor of the protein: $\langle B\rangle_{protein}$ = 28.5 Å^2, $\langle B\rangle_{IMP}$ = 45.4 Å^2, and $\langle B\rangle_{water}$ = 48.5 Å^2. This was not true in the HGPRTase·GMP complex, in which the average temperature factors were about the same for the protein and the ligand ($\langle B\rangle_{protein}$ = 28.5 Å^2, $\langle B\rangle_{GMP}$ = 28.9 Å^2, and $\langle B\rangle_{water}$ = 39.1 Å^2). Since identical refinement strategies were employed for both structures, this difference in average *B* factors probably reflects a real difference in the degree of order of IMP and GMP when bound to HGPRTase. The active site structures are compared in Figure 8.

DISCUSSION

Our study of the kinetic mechanism of human HGPRTase has directly established that the phosphoribosyl transfer step catalyzed by the enzyme is fast and that the rate of the overall reaction in both directions is limited by product release steps. We have documented the existence of a dead-end E·Hx·PP_i complex. Our results demonstrate that release of each product directly from ternary complex is possible for reactions in both directions. However, substrate binding is effectively ordered. This type of mechanism was reported for hexokinase (Wilkinson & Rose, 1979). It is interesting to note that the release of nucleotide and PP_i is largely ordered, with PP_i released first, which is essentially the same as the schistosomal HGPRTase (Yuan *et al.*, 1992).

Table 2 summarizes all K_m, k_{cat}, and K_D values determined here. An updated kinetic mechanism is proposed on the basis of the results reported in this work (Scheme 1 and Table 3) which contains measured or estimated rate constants for all of the individual steps. Guanine-stimulated IMP pyrophosphorolysis revealed that release of PRPP from the E·PRPP complex is partially rate-limiting in the reverse reaction and a rate of 0.24 s^{-1} (k_{-1}) was derived for PRPP dissociation. Knowing $K_{D(PRPP)}$ from equilibrium gel filtration, the second-order rate constant for the binding of PRPP to free enzyme (k_1, 0.20 × 10^6 M^{-1} s^{-1}) was readily obtained and is essentially identical to k_{cat}/K_m (0.17 × 10^6 M^{-1} s^{-1}) for this substrate. The association rate constant for PRPP is several orders of magnitude slower than diffusion-controlled association of enzyme and substrate but is not atypical among enzymes utilizing nucleotides as substrates (Fersht, 1985). A rate of 9.5 s^{-1} (k_{-2}) was calculated for the dissociation of Hx from the E·PRPP·Hx complex on the basis of the overall rate of guanine-stimulated IMP pyrophosphorolysis. The association rate constant for Hx (k_2) was determined to be 1.9 × 10^7 M^{-1} s^{-1} using single-turnover experiments with a molar excess of E·PRPP and was very similar to the value of k_{cat}/K_m (1.3 × 10^7 M^{-1} s^{-1}) for this substrate. Pre-steady state experiments established rapid phosphoribosyl transfer with rate constants of 131 s^{-1} (k_3) and 9 s^{-1} (k_{-3}) in the forward and reverse reactions, respectively. Partitioning of [^{3}H]IMP between its release and [^{3}H]Hx formation (0.62 s^{-1}) in isotope trapping experiments allowed the calculation that IMP is released from the E·PP_i·IMP complex at 12 s^{-1} (k_7). Experiments with added pyrophosphatase indicated that the release of PP_i from E·PP_i·IMP is the main pathway of product release in the forward reaction ($k_4 \gg 12$ s^{-1}). As reasoned below, K_{PP_i} (k_4/k_{-4}) was estimated to be 130 μM; therefore, the rate constant for association of PP_i with the E·IMP complex (k_{-4}) must be at least 0.09 × 10^6 M^{-1} s^{-1}. Since the pre-steady state study demonstrated that product release must be rate-determining for the forward reaction and it was inferred that PP_i release was much faster than the overall rate, it follows that the release of IMP from the E·IMP complex must be rate-limiting (k_5 = 6.0 s^{-1}). The knowledge of $K_{D(IMP)}$, determined by isothermal titration calorimetry, and k_5 allows the rate constant for association of IMP to the free enzyme (k_{-5}) to be estimated to be 0.09

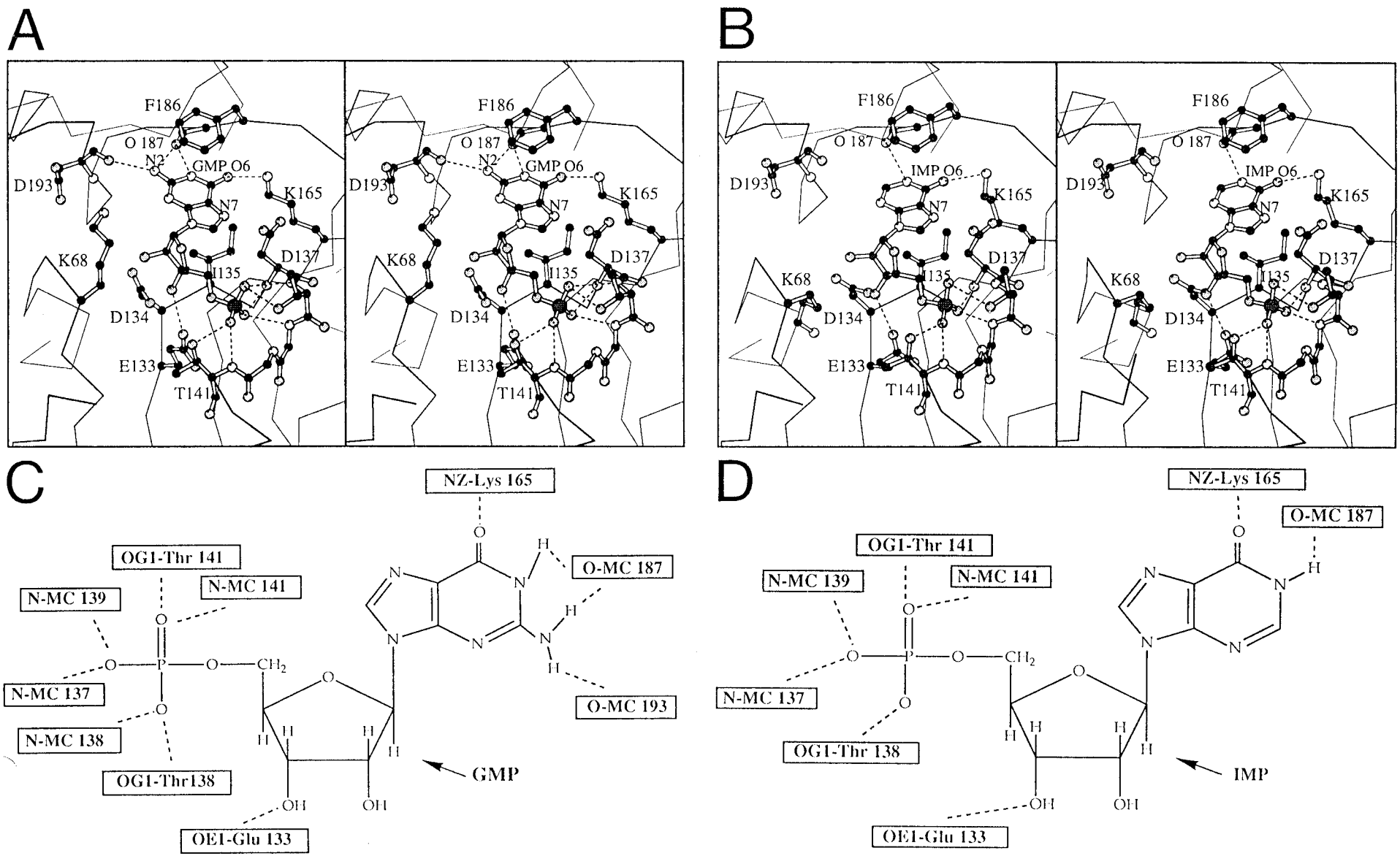

FIGURE 8: Stereodiagrams of the active site of HGPRTase complexed with GMP (A) or IMP (B). The hydrogen bond interactions (<3 Å) between the active site residues and bound GMP and IMP are represented by dashed lines. Schematic diagrams of the hydrogen bond interactions (<3 Å, dashed lines) between the active site residues and bound GMP (C) and IMP (D).

Table 2: Steady State Kinetic Parameters and Binding Equilibrium Constants for HGPRTase[a]

parameter	value	comments
K_m(Hx)	0.45 μM	
K_m(Gua)[b]	3.5 μM	
K_m(PRPP)	31 μM	HPRT reaction
K_m(PRPP)[b]	65 μM	GPRT reaction
K_m(IMP)	5.4 μM	
K_m(PP_i)	25 μM	
k_{cat}(forward)	6.0 s^{-1}	HPRT reaction
k_{cat}(forward)	13 s^{-1}	GPRT reaction
k_{cat}(reverse)	0.17 s^{-1}	IMP pyrophosphorolysis
K_D(PRPP)	1.3 μM	equilibrium gel filtration
K_D(IMP)	61 μM	isothemal titration calorimetry
K_D(GMP)	7.1 μM	isothemal titration calorimetry

[a] All values were determined at 23 °C. [b] These were determined at 30 °C.

$\times 10^6$ M^{-1} s^{-1}, which is comparable to the value of k_{cat}/K_m (0.04×10^6 M^{-1} s^{-1}) for IMP. The rate of the reverse reaction coupled to QAPRTase showed that PRPP dissociates from the E·PRPP·Hx complex with a rate of 0.28 s^{-1} (k_6).

On the basis of the proposed kinetic mechanism (Scheme 2, a simplified version of Scheme 1 which includes only functionally significant steps), the following equations (eqs 5−8) are derived, using the concept of net rate constants (Cleland, 1975) to relate K_m to individual rate constants.

$$K_m(\text{PRPP}) = k_{cat\ (forward)}/k_1 \quad (5)$$

$$K_m(\text{Hx}) = [k_{cat\ (forward)}/k_2](1 + k_{-2}/k'_3) \quad (6)$$

$$K_m(\text{IMP}) = k_{cat\ (reverse)}/k_{-5} \quad (7)$$

$$K_m(\text{PP}_i) = [k_{cat\ (reverse)}/k_{-4}](1 + k_4/k'_{-3}) \quad (8)$$

where k'_3 and k'_{-3} are the net rate constants for k_3 and k_{-3}, respectively. Since most of the individual rate constants were either measured or deduced, it is feasible to use them to calculate the K_m for each substrate according to eqs 5−8 as a test to determine whether the individual rate constants are correct. The calculated K_m values for PRPP, Hx, and IMP were 30, 0.36, and 1.8 μM, respectively. These values are in good agreement with those measured experimentally at room temperature, which are 31 μM for PRPP, 0.45 μM for Hx, and 5.4 μM for IMP. The minimal values for k_4 and k_{-4} do not allow a meaningful calculation of K_m for PP_i, whose measured value was 25 μM.

Table 3: Kinetic Constants for HGPRTase

constant	value	comments
k_1	0.20×10^6 M^{-1} s^{-1}	$k_{-1}/K_{D(PRPP)}$
k_{-1}	0.24 s^{-1}	rate-limiting step in the reverse reaction
k_2	1.9×10^7 M^{-1} s^{-1}	experimentally determined
k_{-2}	9.5 s^{-1}	rate-limiting step in the reverse reaction
k_3	131 s^{-1}	determined from a pre-steady state study
k_{-3}	9 s^{-1}	determined from a pre-steady state study
k_4	>12 s^{-1}	main product release pathway
k_{-4}	$>0.09 \times 10^6$ M^{-1} s^{-1}	$k_4/K_{D(PP_i)}$
k_5	6.0 s^{-1}	rate-limiting step in the forward reaction
k_{-5}	0.09×10^6 M^{-1} s^{-1}	$k_5/K_{D(IMP)}$
k_6	0.28 s^{-1}	determined from the reverse reaction coupled to QAPRTase
k_7	12 s^{-1}	derived from an isotope trap experiment

We were unable to detect binding of either Hx or PP_i to apoenzyme, setting minimal values of about 2 mM for their K_Ds. Our observation that the presence of PP_i did not affect either binding or isotope trapping of [β-^{32}P]PRPP also supported the conclusion that the K_D for PP_i is very high. However, we observed competitive inhibition by PP_i with respect to PRPP (K_I = 240 μM), confirming previously reported data (Giacomello & Salerno, 1978). These observations suggest that a dead-end E·Hx·PP_i complex must be able to form, a deduction confirmed by the detection of [^{32}P]-PP_i binding in the presence of 2.2 mM Hx. The order of binding leading to dead-end complex formation was not established.

Several features of the kinetic mechanism serve to explain the very slow rate of the reverse reaction, the difficulty observing it without XO, and its stimulation (rather than inhibition) by guanine. First among these features is the slow release of PRPP from either E·PRPP (0.24 s^{-1}) or E·PRPP·Hx (0.28 s^{-1}) complexes. As discussed below, this slow release may be a function of a rate-limiting movement of a peptide loop. The second feature limiting the rate of IMP pyrophosphorolysis is the rapid (1.9×10^7 M^{-1} s^{-1}) and tight

Scheme 1

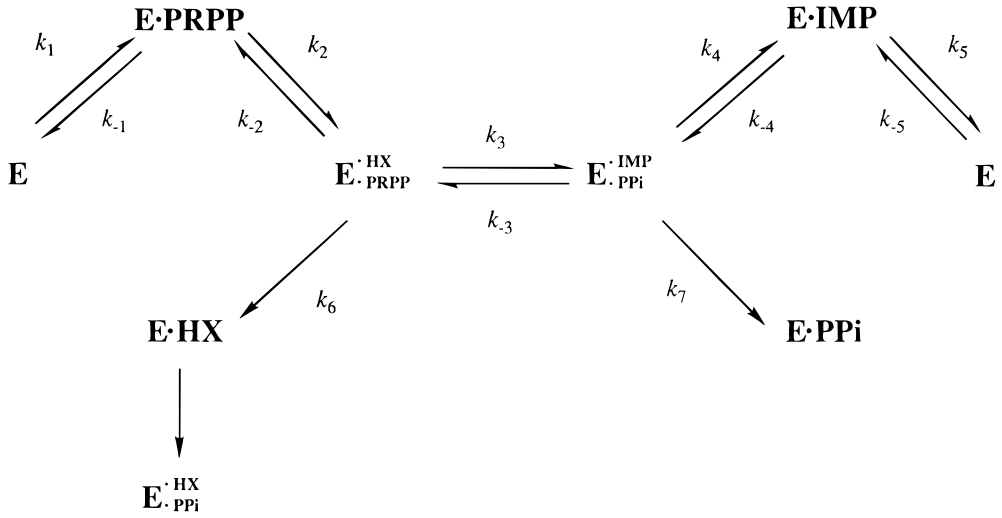

Scheme 2

$$\mathrm{E} \underset{k_{-1}}{\overset{k_1}{\rightleftharpoons}} \mathrm{E{\cdot}PRPP} \underset{k_{-2}}{\overset{k_2}{\rightleftharpoons}} \mathrm{E}\cdot{}^{\mathrm{HX}}_{\mathrm{PRPP}} \underset{k_{-3}}{\overset{k_3}{\rightleftharpoons}} \mathrm{E}\cdot{}^{\mathrm{IMP}}_{\mathrm{PPi}} \underset{k_{-4}}{\overset{k_4}{\rightleftharpoons}} \mathrm{E{\cdot}IMP} \underset{k_{-5}}{\overset{k_5}{\rightleftharpoons}} \mathrm{E}$$

($K_D = 0.50\ \mu$M) binding of Hx to E·PRPP complexes. Even at 1 μM Hx, its rebinding to E·PRPP (19 s^{-1}) is nearly 100 times faster than dissociation of the E·PRPP complex. When overall reverse catalysis is performed in the presence of Hx, with QAPRTase added to remove free PRPP, the overall reaction must thus proceed by PRPP release from the ternary E·PRPP·Hx complex. As proposed by Salerno and Giacomello (1979), the rapid rebinding of base to the E·PRPP complex also explains the action of guanine in stimulating the pyrophosphorolysis of IMP. The cellular significance of the base-stimulated pyrophosphorolysis of nucleotides is unclear.

The external K_{eq} for the forward HGPRTase reaction was calculated as the product of the internal equilibrium constants for the five individual reaction steps (Scheme 2). $K_{PP_i}(k_4/k_{-4})$ was not directly determined in our study. However, this value was estimated to be 130 μM on the basis of eq 8. The calculated external K_{eq} was 1.6×10^5, consistent with the observed K_{eq} (1.8-4.3 $\times$ 10^5). This range of values is well above those known for other PRTases. It is well established that the PP_i−ribose 5-phosphate bond of PRPP is of high energy. $\Delta G^{\circ\prime}$ for hydrolysis of the PP_i moiety from PRPP is −8.4 kcal/mol (Frey & Arabshahi, 1995). This value, in conjunction with K_{eq} for phosphoribosyl transfer reactions, yields free energies ($\Delta G^{\circ\prime}$) for nucleosidic bond hydrolysis of OMP, NAMN, AMP, and IMP of −9.76, −8.64, −5.03, and −1.33 kcal/mol, respectively.

Using the rate and equilibrium constants for each individual step, we were able to construct the free energy profile for both forward and reverse reactions catalyzed by human HGPRTase under standard conditions (Figure 9). The free energy difference between substrates (PRPP and Hx) and products (IMP and PP_i) in solution is quite large (7 kcal/mol) compared to that when they are all bound to the enzyme (1.6 kcal/mol). The E·PRPP·Hx complex is stabilized by 16.4 kcal/mol, whereas the E·PP_i·IMP complex is stabilized by 11 kcal/mol, causing the ternary complexes to be nearly isoenergetic, and permitting rapid phosphoribosyl transfer in both the forward and reverse reactions. The energy barrier for the transition state is 15 and 16.6 kcal/mol in the forward and reverse reactions, respectively, which is lower than the energy barrier for the release of PRPP from the E·PRPP·Hx complex (18.5 kcal/mol).

The kinetic results in this paper can be related to the two known three-dimensional structures of human HGPRTase−nucleotide complexes (Eads *et al*., 1994; results reported in this paper). The calorimetric data show that GMP binds 10-fold more strongly than IMP ($K_D = 7$ and 61 μM for GMP and IMP, respectively). The enthalpy of binding of GMP is more favorable than that of IMP by 6.5 kcal/mol, probably due to the hydrogen bonds made between the additional exocyclic amino group of GMP and the main chain carbonyls O187 and O193 of the enzyme. However, the more favorable enthalpy of GMP binding is partially offset by a less favorable entropy of binding. The crystal structure of the HGPRTase·IMP complex did not reveal an ordered water molecule in the position that would be occupied by the GMP N2 amine. This finding is consistent with the observation that binding of GMP is not more entropically favorable than binding of IMP, but it does not explain why GMP binding is less entropically favorable. The crystal structure of both complexes indicated that IMP may be more disordered when bound, as reflected in the higher *B*-factors of the ligand as compared to the average protein *B*-factors. The lack of the N2 amino group in IMP results in a less sterically constrained fit of the ligand to the protein, and the extra flexibility

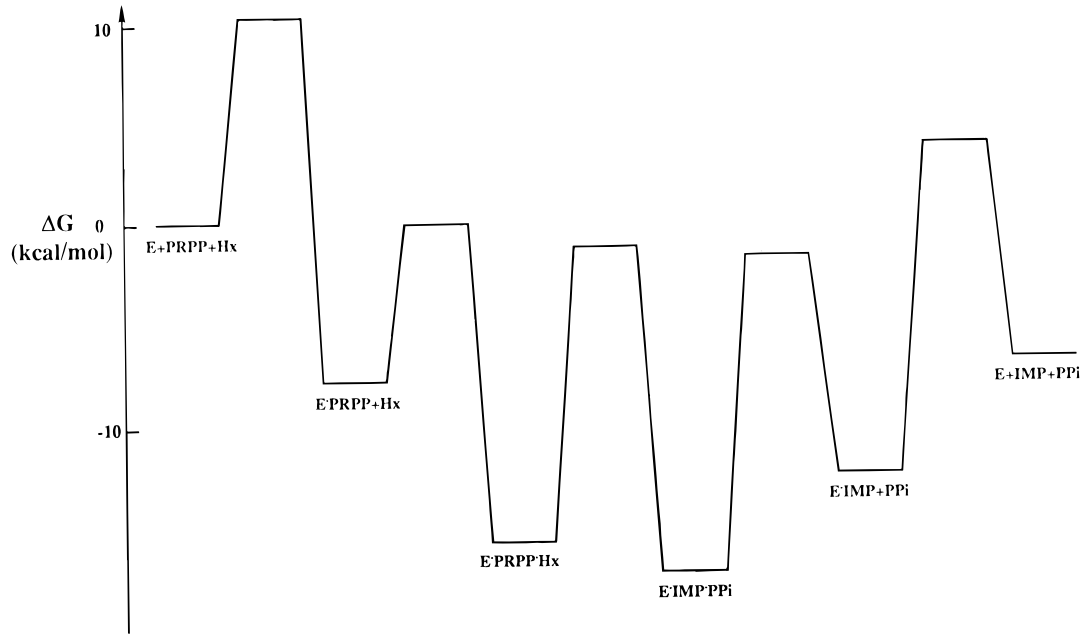

FIGURE 9: Free energy profile for HGPRTase-catalyzed reactions. The energy barrier between E·IMP·PP_i and E·IMP+PP_i could be smaller than shown since lower limits for rate constants involved were used in calculating the energy barrier.

allowed should be reflected to some degree in the less unfavorable entropy of binding. In addition, it is possible that differences in the solution structures of GMP and IMP, in particular the *syn*/*anti* ratio, might contribute to differences in the entropy of binding to HGPRTase.

In both structures, the active site is accessible from solution, suggesting that binding of substrates might be random. The ribose portion of the nucleotide is the most solvent-exposed (40 $Å^2$ solvent accessible area), whereas the base is relatively buried in a solvent inaccessible cavity. The exact position of PP_i in the ternary complexes has not been determined. However, on the basis of the position of ribose C1′, it is likely that the PP_i group would also be fairly solvent-exposed, and there would not need to be a large conformational change required for PP_i release. Deductions from the nucleotide complexes must be tempered by the proposal (Eads *et al*., 1994) of two structural changes occurring on substrate binding and catalysis. (1) The anti-parallel β sheet containing B8 and B9 might deform upon base binding, an event that could be slow or energetically unfavorable. (2) A flexible loop (residues 103−117), adjacent to the active site, may move to block access of solvent to the transition state.

On the basis of the structures of the nucleotide complexes, it might be expected that base would bind first to the enzyme, as it occupies the more buried site, to which access would be restricted if the ribose group of PRPP occupied the same position identified for the ribose group of GMP. However, kinetic data show clearly that PRPP binds before Hx. It is difficult to reconcile these observations without proposing some movement of enzyme or bound substrate. A large displacement of the ribose 5-phosphate group has been documented in OPRTase in complexes with OMP and with PRPP (Scapin *et al*., 1994, 1995). Conformational changes have also been implicated from the behavior of a PRPP analog with glutamine amido phosphoribosyltransferase (Kim *et al*., 1995), an enzyme that shares extensive structural similarity with HGPRTase. Far more extensive conformational changes have recently been proposed for HGPRTases, on the basis of covalent modification studies with dialdehyde GMP (Kanaani *et al*., 1995), but the proposed changes are difficult to reconcile with known structural information.

Our structural and kinetic observations with HGPRTase may have general application to other PRTases. Specifically, in OPRTase, a homologous flexible loop contains essential residues and moves into the active site during catalysis (Ozturk *et al*., 1995a,b; Scapin *et al*., 1995). Such movement was proposed to be necessary to protect a documented oxocarbonium-like transition state (Tao *et al*., 1996). In OPRTase, the structure of an enzyme·SO_4 complex has permitted the visualization of the loop in a "closed" or "down" position (Henriksen *et al*., 1996), an important step toward understanding the specific roles of loop residues. As with HGPRTase, it appears that protein conformational events may participate in the kinetic mechanism and may determine the rate of product release. The determination of additional PRTase structures that capture further structural events in catalysis is both timely and important.

ACKNOWLEDGMENT

We thank Mr. Edy Segura of the Fels Protein Facility for protein sequencing and Dr. Vern Schramm for commenting on an early version of the manuscript. We thank Drs. Barbara Stitt and David Ash for reading the manuscript and making useful suggestions. We gratefully acknowledge the Wistar Protein Microchemistry Core Facility for performing the quantitative amino acid analysis. We would also like to thank Lisa Lorigan and Dr. David Speicher for their excellent assistance. We thank two anonymous reviewers for their careful analysis and suggestions on our manuscript.

REFERENCES

Ali, L. Z., & Sloan, D. L. (1982) *J. Biol. Chem. 257*, 1149−1155.
Bell, R. M., & Koshland, D. E., Jr. (1970) *Biochem. Biophys. Res. Commun. 38*, 539−545.
Bhatia, M. B., Vinitsky, A., & Grubmeyer, C. (1990) *Biochemistry 29*, 10480−10487.
Brashear, W. T., & Parsons, S. M. (1975) *J. Biol. Chem. 250*, 6885−6890.
Cho, Y. K., Matsunaga, T. O., Kenyon, G. L., Bertagnolli, B. L., & Cook, P. F. (1988) *Biochemistry 27*, 3320−3325.
Chou, Y. J., & Martin, R. G. (1972) *J. Bacteriol. 112*, 1010−1013.
Cleland, W. W. (1975) *Biochemistry 14*, 3220−3224.
Cleland, W. W. (1979) *Methods Enzymol. 63*, 103−139.
de Groodt, A., Whitehead, E. P., Heslot, H., & Poirier, L. (1971) *Biochem. J. 122*, 415−420.
Dovey, H. F., McKerrow, J. H., & Wang, C. C. (1984) *Mol. Biochem. Parasitol. 11*, 157−168.
Dovey, H. F., McKerrow, J. H., Aldrit, S. M., & Wang, C. C. (1986) *J. Biol. Chem. 261*, 944−948.
Eads, J., Scapin, G., Xu, Y., Grubmeyer, C., & Sacchettini, J. C. (1994) *Cell 78*, 325−334.
Ebert, R. F. (1986) *Anal. Biochem. 154*, 431−435.
Fersht, A. (1985) *Enzyme Structure and Mechanism*, Freeman, New York.
Frey, P. A., & Arabshahi, A. (1995) *Biochemistry 34*, 11307−11310.
Giacomello, A., & Salerno, C. (1978) *J. Biol. Chem. 253*, 6038−6044.
Groth, D. P., & Young, C. G. (1971) *Biochem. Biophys. Res. Commun. 43*, 82−87.
Grubmeyer, T. C., Chu, K.-W., & Insinga, S. (1987) *Biochemistry 26*, 3369−3373.
Henderson, J. F., Brox, L. W., Kelley, W. N., Rosenbloom, F. M., & Seegmiller, J. E. (1968) *J. Biol. Chem. 243*, 2514−2522.
Henriksen, A., Aghajari, N., Jensen, K. F., & Gajhede, M. (1996) *Biochemistry 35*, 3803−3809.
Hill, D. L. (1970) *Biochem. Pharmacol. 19*, 545−557.
Hochstadt, J. (1978) *Methods Enzymol. 51*, 549−558.
Holden, J. A., & Kelley, W. N. (1978) *J. Biol. Chem. 253*, 4459−4463.
Hori, M., & Henderson, J. F. (1966) *J. Biol. Chem. 241*, 3404−3408.
Hove-Jensen, B., Harlow, K. W., King, C. J., & Switzer, R. L. (1986) *J. Biol. Chem. 261*, 6765−6771.
Hughes, K. T., Dessen, A., Gray, J. P., & Grubmeyer, C. (1993) *J. Bacteriol. 175*, 479−486.
Hummel, J. P., & Dreyer, W. J. (1962) *Biochim. Biophys. Acta 63*, 530−532.
Jolly, D. J., Okayama, H., Berg, P., Esty, A. C., Filpula, D., Bohlen, P., Johnson, G. G., Shively, J. E., Hunkapillar, T., & Friedmann, T. (1983) *Proc. Natl. Acad. Sci. U.S.A. 80*, 477−481.
Jones, T. A. (1985) *Methods Enzymol. 115*, 157−171.
Kalckar, H. M. (1947) *J. Biol. Chem. 167*, 429−443.
Kanaani, J., Maltby, D., Forcia, P., & Wang, C. C. (1995) *Biochemistry 34*, 14987−14996.
Kelley, W. N., Rosenbloom, F. M., Henderson, J. F., & Seegmiller, J. E. (1967) *Proc. Natl. Acad. Sci. U.S.A. 57*, 1735−1739.
Keough, D. T., Emmerson, B. T., & de Jersey, J. (1991) *Biochim. Biophys. Acta 1096*, 95−100.
Kim, J. H., Wolle, D., Haridas, K., Parry, R. J., Smith, J. L., & Zalkin, H. (1995) *J. Biol. Chem. 270*, 17394−17399.
Korn, E. D., Remy, C. N., Wasilejko, H. C., & Buchanan, J. M. (1955) *J. Biol. Chem. 218*, 875−883.

Kornberg, A., Liberman, I., & Simms, E. S. (1955) *J. Biol. Chem. 215*, 417−427.
Krenitsky, T. A., & Papaioannou, R. (1969) *J. Biol. Chem. 244*, 1271−1277.
Lesch, M., & Nyhan, W. L. (1964) *Am. J. Med. 36*, 561−570.
Martin, R. C. (1963) *J. Biol. Chem. 238*, 257−268.
Miller, R. L., Ramsey, G. A., Krenitsky, T. A., & Elion, G. B. (1972) *Biochemistry 11*, 4723−4731.
Muensch, H., & Yoshida, A. (1977) *Eur. J. Biochem. 76*, 107−112.
Natalini, P., Santarelli, I., Rugguierri, S., Vita, A., & Magni, G. (1979) *J. Biol. Chem. 254*, 1558−1563.
Nilsson, D., & Lauridsen, A. A. (1992) *Mol. Gen. Genet. 235*, 359−364.
Ogasawara, N., Makai, S., & Yoshikawa, H. (1994) *DNA Res. 1*, 1−14.
Olsen, A. S., & Milman, G. (1977) *Biochemistry 16*, 2501−2505.
Ozturk, D. H., Dorfman, R. H., Scapin, G., Sacchettini, J. C., & Grubmeyer, C. (1995a) *Biochemistry 34*, 10755−10763.
Ozturk, D. H., Dorfman, R. H., Scapin, G., Sacchettini, J. C., & Grubmeyer, C. (1995b) *Biochemistry 34*, 10764−10770.
Parkin, D. W., Leung, H. B., & Schramm, V. L. (1984) *J. Biol. Chem. 259*, 9411−9417.
Purich, D. L., & Allison, R. D. (1983) in *Contemporary Enzyme Kinetics and Mechanism*, pp 403−446, Academic Press, New York.
Queen, S. A., Jaght, D. V., & Reyes, P. (1988) *Mol. Biochem. Parasitol. 30*, 123−134.
Reyes, P., Rathod, P. K., Sanchez, D. J., Mrema, J. E. K., Rieckman, K. H., & Heidrich, H.-G. (1982) *Mol. Biochem. Parasitol. 5*, 275−290.
Rose, I. A. (1980) *Methods Enzymol. 64*, 47−59.
Rose, I. A. (1995) *Methods Enzymol. 249*, 315−340.
Salerno, C., & Giacomello, A. (1979) *J. Biol. Chem. 254*, 10232−10236.
Salerno, C., & Giacomello, A. (1981) *J. Biol. Chem. 256*, 3671−3673.
Scapin, G., Grubmeyer, C., & Sacchettini, J. C. (1994) *Biochemistry 33*, 1287−1294.
Scapin, G., Ozturk, D. H., Grubmeyer, C., & Sacchettini, J. C. (1995) *Biochemistry 34*, 10744−10754.
Scatchard, G. (1949) *Ann. N. Y. Acad. Sci. 51*, 660−672.
Seegmiller, J. E., Rosenbloom, F. M., & Kelley, W. N. (1967) *Science 155*, 1682−1684.
Segel, I. H. (1975) *Enzyme Kinetics*, pp 813−818, Wiley, New York.
Senft, A. W., & Crabtree, A. (1983) *Pharmacol. Ther. 20*, 341−356.
Somoza, J. R., Chin, M. S., Forcia, P. J., Wang, C. C., & Fletterick, R. J. (1996) *Biochemistry 35*, 7032−7040.
Stout, J. T., & Caskey, C. T. (1985) *Annu. Rev. Genet. 19*, 127−148.
Stout, J. T., & Caskey, C. T. (1989) in *The Metabolic Basis of Inherited Disease* (Scriver, C. R., Beaudet, A. L., Sly, W. S., & Valle, D., Eds.) pp 1007−1028, McGraw-Hill, New York.
Tao, W., Grubmeyer, C., & Blanchard, J. S. (1996) *Biochemistry 35*, 14−21.
Tronrud, D. E., Ten Eyck, L. F., & Mathews, B. W. (1988) *Acta Crystallogr., Sect. A 43*, 489−501.
Tuttle, J. V., & Krenitsky, T. A. (1980) *J. Biol. Chem. 255*, 909−916.
Ullman, B., & Carter, D. (1995) *Infect. Agents Dis. 4*, 29−40.
Victor, J., Greenberg, L. B., & Sloan, D. L. (1979) *J. Biol. Chem. 254*, 2647−2655.
Vinitsky, A., & Grubmeyer, C. (1993) *J. Biol. Chem. 268*, 26004−26010.
Wilkinson, K. D., & Rose, I. A. (1979) *J. Biol. Chem. 254*, 12567−12572.
Wilson, J. M., Tarr, G. E., Mahoney, W. C., & Kelley, W. N. (1982) *J. Biol. Chem. 257*, 10978−10985.
Yuan, L., Craig, S. P., III, McKerrow, J. H., & Wang, C. C. (1992) *Biochemistry 31*, 806−810.

BI9616007